VI International Conference on Computational Methods in Marine Engineering
MARINE 2015
F. Salvatore, R. Broglia and R. Muscari (Eds)

EXPERIMENTAL TEST AND NUMERICAL SHAPE OPTIMIZATION OF A POINT PIVOTED ABSORBER FOR WAVE ENERGY CONVERSION

D. COIRO[1], G. TROISE[2], G. CALISE[*] AND N. BIZZARRINI[1]

[*] Department of Industrial Engineering – Aerospace Division,
University of Naples "Federico II", 80125 Naples, Italy
e-mail: g.calise@email.it, web page: http://www.adag.unina.it/

[1] Department of Industrial Engineering – Aerospace Division,
University of Naples "Federico II", 80125 Naples, Italy
web page: http://www.adag.unina.it/

[2] Seapower Scarl, Consortium with University of Naples "Federico II"
Via Giuseppe Fiorelli 14, 80121 Naples, Italy
web page: http://www.seapowerscrl.com/

Key words: wave energy conversion, point pivoted absorber, buoy, energy from waves

Abstract. This paper presents a numerical study on an innovative system for converting energy from waves. It consists of a point pivoted body which oscillates in presence of waves. The system uses a linear electrical generator which converts floating movements of the buoyant body into electrical power. The buoyant body floats, describing an arc, by means of two hinges. A suitable Power Take-off Device (PTO) is placed between buoy support arms and the fixed structure and has the function to convert the mechanical power of the linear oscillating motion of the connecting piston into electrical power. A design assumption is made on the PTO control system: PTO reaction force is assumed to be linearly dependent on piston oscillation velocity with a given force-speed gain. This coefficient is strictly connected to electrical generator characteristics and its value has an effect on power conversion efficiency . A scaled model of this system has also been tested in the wave/towing tank facility of Department of industrial Engineering (DII) of University of Naples "Federico II". A variety of numerical analyses, such as potential flow simulations and Unsteady Reynolds Averaged Navier-Stokes (URANS) simulations, have been performed to predict the system performances. Numerical and experimental analyses have included the performances of the baseline geometry, both in free response and under wave excitation, in order to characterize the response of the system, and results have been used to understand which parameters affect more the power production. Finally a numerical optimization procedure has been carried out to optimize the shape of the converter with the final objective of increasing the generated power, eventually imposing a constraint on the amount of immersed volume. In this way, a modified configuration has been predicted with higher power output and the same value of submerged volume, but with different shape.

1 INTRODUCTION

Harvesting energy from waves represents an attractive field of business for several

renewable energy companies. This kind of renewable energy source has numerous advantages with respect to other ones: relatively limited environmental impact and more predictable behavior are very attractive key points for designing a properly working energy system. It is known that ocean wave's characteristics depend on specific installation site and are often quite repeatable in terms of amplitude and frequency.

In the design of a device to extract energy from waves many configuration parameters are involved, such as buoyant body shape, overall system arrangement and type of energy conversion system. This work refers to an innovative system configuration of suitable body shape and system arrangement effects are investigated in order to optimize the energy conversion system too. This kind of system is mainly intended for installation in suitable sea coastal areas. Its operating principle ensures constructive simplicity and ease of operation. On the other hand a proper linear electrical conversion system is also needed.

This work will also present for purposes of comparison with numerical analysis an experimental study of the power performance characteristic of a small scale model of the system, under different operating conditions [1]. A first attempt to optimize the buoy shape, in order to improve power extraction, will be also shown. This work contains, as a first stage, an analytical study of the system for determining its kinematic operating laws. Then, several computer aided simulations, mainly potential flow simulations, are performed for identifying the set of parameters with better performances. Finally, wave/towing tank tests data are used as reference to verify data from simulations, to better set-up the engineering process and to investigate other different combinations as well. The overall workflow and results for selected ocean wave conditions will be shown in the present work.

2 DESCRIPTION OF THE SYSTEM

The primary system configuration is represented in Figure 1. It consists of a floating body linked to a fixed frame by means of two hinges, which allow rotation of the body with respect to the frame, and a point pivoted PTO (Power Take Off) device.

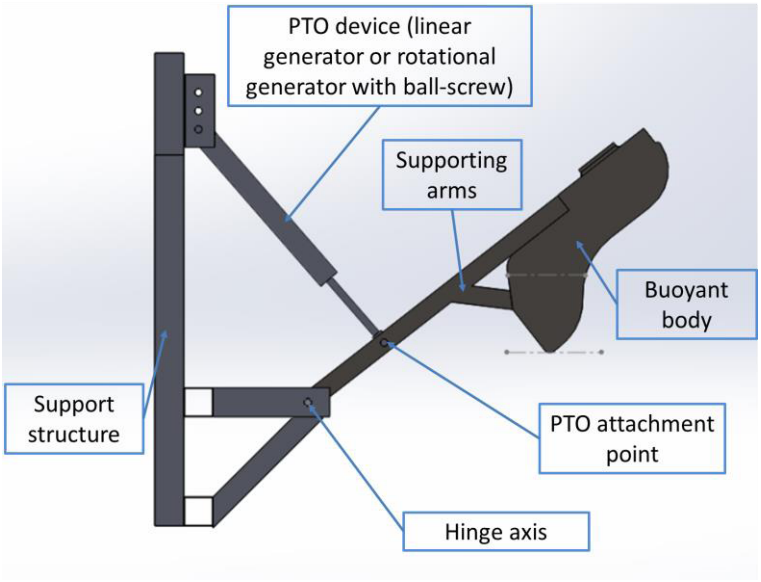

Figure 1: Schematic of the system

The action of the waves results in a rotational motion of the buoy around the submerged hinges, which the buoy is connected to, by means of the support arms. The Power Take Off (PTO) system is represented by a device able to convert the rotational oscillation of the buoy into electrical energy. A suitable device is linked on one side to the fixed structure and on the other to the buoy support arm; the oscillating motion of the device, generated by the wave action on the buoy, may be used for energy conversion, by means of a linear generator or a conventional rotational generator with a ball-screw.

The dynamic behavior of the system may be described to a first order of approximation by the use of a simple equivalent 1DOF equation that represents the equilibrium of moments around the hinge axis:

$$I\ddot{\theta} + B\dot{\theta} + k\theta = M_{ext} + M_{PTO} \tag{1}$$

where:

- I is the rotational inertia around the hinge axis accounting for the hydrodynamic added mass also;
- B is a linear damping coefficient accounting for part of the radiation force, which should be corrected for viscous contribution;
- k is a coefficient related to hydrostatic stiffness;
- M_{ext} is the external moment due to waves excitation forces (diffractive and Froude Krylov forces);
- M_{PTO} is the moment due to the point pivoted power take-off device (PTO);

- θ is the inclination angle of the support arm of the body.

It has to be noted that the effective hydrostatic action is a non-linear function of the instantaneous inclination angle related to the actual shape of the body and the instantaneous wetted surface. On the other hand, the equation with constant coefficient is valid for a regular wave with a single frequency component and should be written in the frequency domain. Particularly, for irregular waves, the radiation forces should be treated in a more rigorous way using the convolution integral and the impulsive response function. The simulation codes used in hydrodynamic analyses take into account the instantaneous hydrostatic and Froude-Krylov forces associated with the effective wetted surface and may use the convolution method to deal with the radiation forces.

The PTO device is built up by an electromechanical conversion system with an oscillating telescopic piston that is linked on one end to the support arm, and at the other end is pivoted to the support structure. A suitable control system has to be implemented in the PTO device, in order to ensure that the force response of the device comply with a given control law. The selected PTO system was controlled so as to produce a force response proportional to velocity variations (Eq. 2).

$$F_{pist} = k_V * V_{pist} \tag{2}$$

where k_V is an adjustable gain, F_{pist} is the PTO force acting on the oscillating piston of the PTO, and V_{pist} is the elongation velocity of the piston. The gain coefficient k_V may influence the overall behavior of the system in response to wave action and may affect power conversion performances. The power extracted by the conversion system, may be evaluated as:

$$P = F_{pist} * V_{pist} = k_V * V_{pist}^{\ 2} \tag{3}$$

It has to be noted that the choice of the type of control law and strategy itself is an important step in the design process. In this case a linear relation has been implemented for simplicity, but other control strategies may in principle offer better performances.

3 POTENTIAL FLOW SIMULATIONS

A numerical model based on a potential flow theory has been developed. Several simulations have been performed by the use of a boundary elements code in order to estimate hydrodynamic coefficients and, then, solve the time domain equations of motion: in this way, it is possible to evaluate the dynamic response of the system to external forces, complying with the applied constraints.

For the analysis, a commercial code named AQWA has been used. AQWA is a numerical code for hydrodynamic calculations included in the ANSYS suite. AQWA has different operating capabilities: the hydrodynamic diffraction and radiation coefficients are calculated for each configuration using a boundary element method based on distribution of sources; on the other hand, the code is able to perform a time simulation and to account for 6 degrees of freedom body motion complying with constraints. This code has been used in cooperation with the “Polytechnic University of Turin”.

Hydrodynamic coefficients such as added mass, radiation damping and diffractive forces were evaluated as a function of frequency, based upon a linearization around the initial

equilibrium condition.

In the performed simulations only the buoy shape has been considered neglecting the presence of the submerged part of the support arms.

Using a diffused approach, the simulation of wave-body interaction is decomposed in the solution of different boundary value problems, assuming that a superposition principle may be applied. The potential solution is written as the sum of different terms: a) the undisturbed wave field (related to Froude-Krylov forces), b) the perturbation field due to the presence of the body (related to diffraction forces), c) the radiation field due to the wave radiated by the body motion in a steady free surface (related to radiation forces expressed in terms of added mass and radiation damping). Each problem is solved separately with its own boundary condition.

The general boundary conditions express the non-penetration condition of the flow on the body wall and on the seabed, and the free surface conditions (constant pressure outside the fluid on the free surface and permanence of a particle on the free surface). In a first order approximation, which leads to the Airy linear wave theory, the free surface boundary conditions, which in general involves a non-linearity, related to the fact that the free surface shape is unknown a priori, may be linearized applying such condition at the still water level. On the other hand, in solving the diffraction and radiation problems the wall boundary condition may be linearized imposing such condition always on the initial equilibrium condition, neglecting the variation of the wetted surface due to the effects of the real free surface shape and of the body motion [4].

In the performed simulations only the Airy linear regular wave theory has been used. The code used treats the diffraction and radiation problem by the linearized approach. Froude-Krylov and hydrostatic forces, on the other hand, have been treated in a non-linear way in the time domain, by integrating at each simulation time-step the pressure field on the effective wetted surface of the body.

The results reported in this section are related to a scaled model that has been tested in the wave/towing tank of the Department of Industrial Engineering (DII) of University of Naples “Federico II”. As an example of the calculation results some of the hydrodynamic coefficients are reported in the Figure 2.

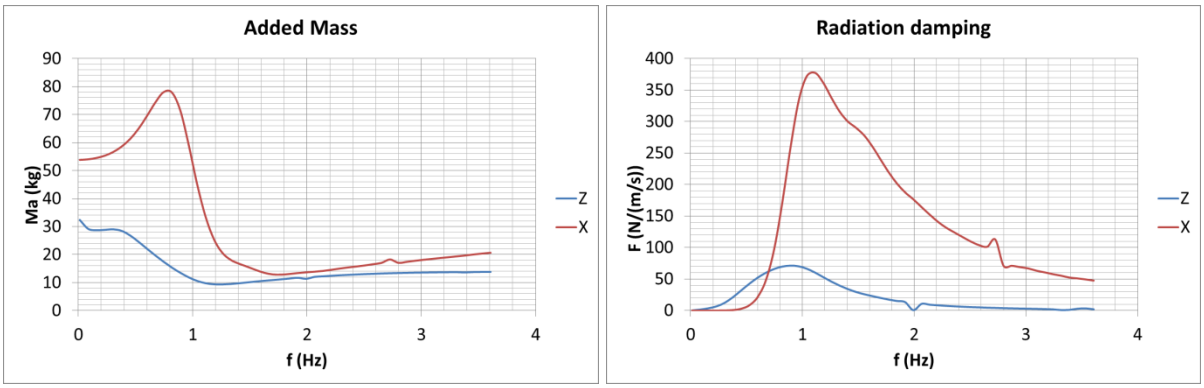

Figure 2: Added mass and radiation damping as a function of frequency

Some irregular frequencies may be observed. Such irregular values are due to known

numerical issues, but the frequencies at which such problems appear are relatively far from the frequency of interest (near the resonance at about 0.8 Hz). On the other hand, hydrostatic and Froude-Krylov forces are evaluated nonlinearly during time integration accounting for the effective wetted surface of the body.

In order to simulate the dynamic response of the system in the time domain, the presence of the PTO device is also accounted for by applying a control force, as described in the equation (2). The non-linearity associated with the kinematic of the linking system is accounted for in the model. This task is accomplished, in the code used for the calculation, by introducing an external force defined as a function of the actual piston extension velocity.

4 NUMERICAL-EXPERIMENTAL COMPARISON

A set of tests was carried out on a scale model in order to assess the response of the system and for comparison purposes with numerical simulations. The test campaign performed at the University of Naples had the purpose to investigate the overall behavior of the system, particularly in terms of power output. Tests were performed at the wave/towing tank of the DII. This facility has a wave generator capable of producing waves with variable frequency and amplitude. Tested model main properties are listed in Table 1.

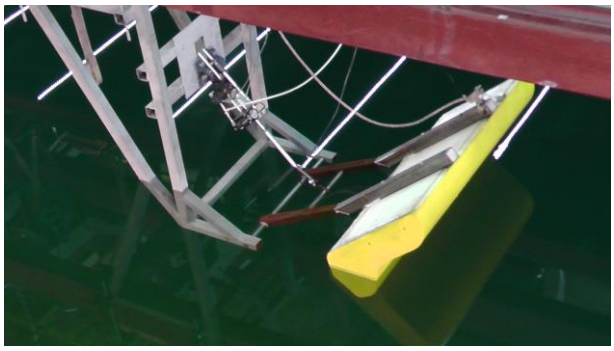

Figure 3: Small scale model installed in naval towing tank of the University of Naples

Table 1: Scaled model properties

Body height	0.6	m
Body width	1	m
Body weight	32.5	kg
Hinge moment (Body + arms)	21.65	kg m^2
Draft	0.2	m
Body section @ water level	0.21	m^2
Immersed volume	0.0325	m^3

During this tests the PTO device was simulate using a controlled pneumatic actuator used as a power absorber.

A first set of preliminary test has been performed; in the following figure an observed free decay test is reported.

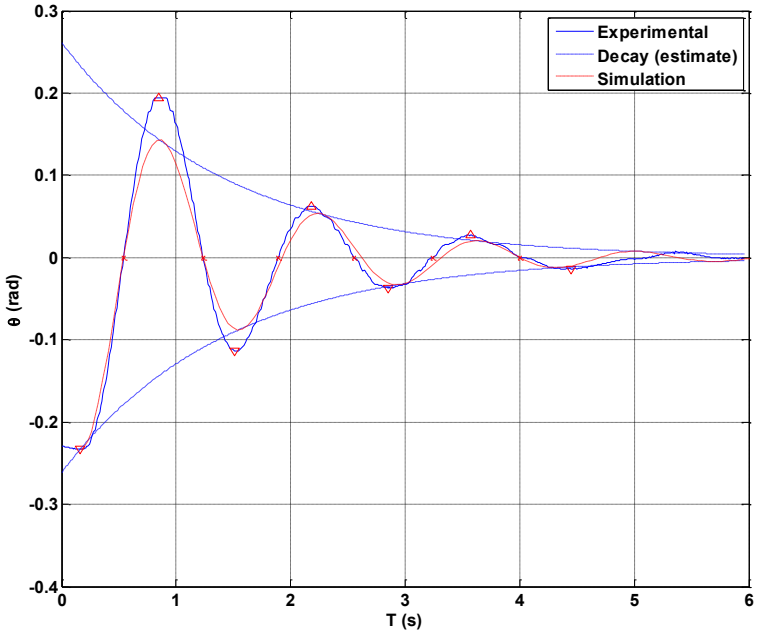

Figure 4: Free decay experimental test. (The line indicated as simulation refers to a simple linear simulation performed just for comparison purposes)

Although some problems was encountered due to the small number of oscillations and to difficulties in controlling the starting values, some results about the natural damped oscillation have been obtained and reported in the following Table 2.

Table 2: Free damped response characteristics (mean values)

	Damping ratio	Natural frequency
	ζ (-)	f_n (Hz)
Mean	0.156	0.767
Std. dev.	0.012	0.020

In relation to this preliminary analysis, a simulation of the free response of the system was performed to identify its natural frequency. A frequency of about 0.8 Hz has been observed. Such value is in relatively good agreement with observed test values.

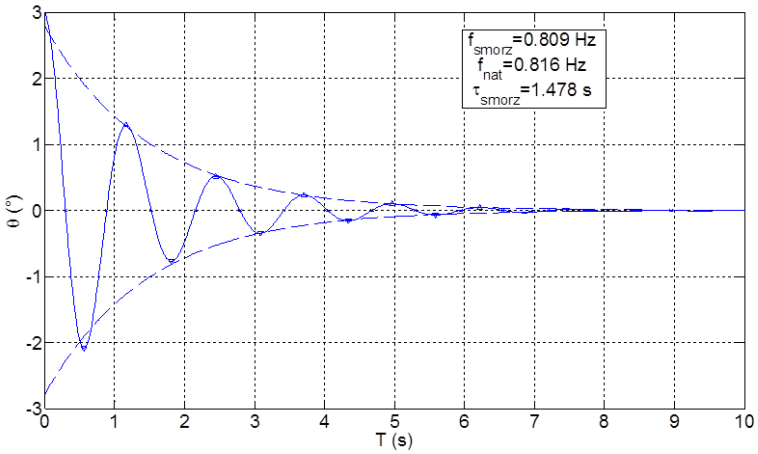

Figure 5: Simulated free damped oscillation (inclination angle)

At a second stage, absorber effects were introduced into numerical analyses as well. Then, other simulations were performed using the full model subject to the excitation of linear regular waves (in conditions similar to those tested in the wave/towing tank).

In Figure 6 and Figure 7, some comparisons between simulated and experimental time histories are reported for a test case near to resonance conditions.

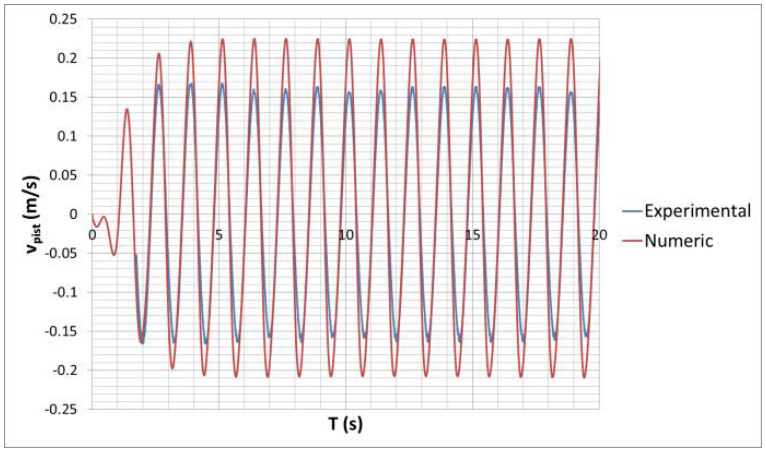

Figure 6: Numerical (potential theory) - experimental comparison. Piston velocity time histories. (f=0.8 Hz, K= 570 N/(m/s))

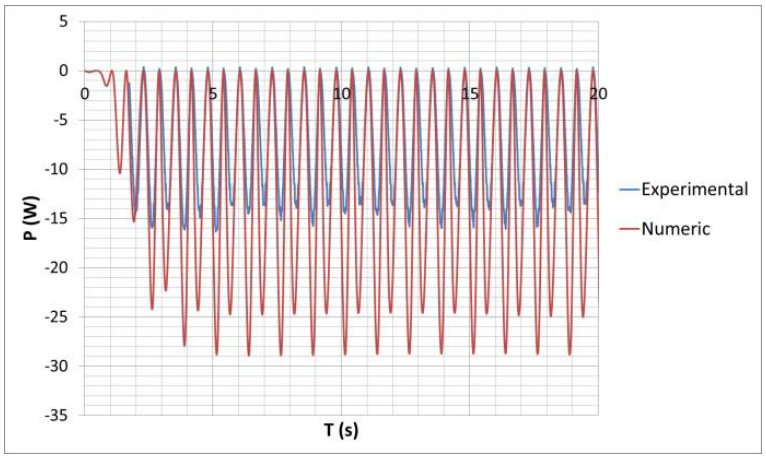

Figure 7: Numerical (potential theory) - experimental comparison. Instantaneous power time histories. (A=0.05 m, f=0.8 Hz, K= 570 N/(m/s))

Numerical potential flow data compared to experimental tests have shown to be in relatively good agreement with respect to natural frequency and wave frequency for max power (mean and instantaneous), but the value of the power from simulations is almost double of experimental one. Part of this issue is probably related to an overestimation of the velocity, and thus of the force at the absorber, in the simulations, since no viscous effects were introduced.

The numerically simulated average power output, in a condition with wave amplitude of 5 cm and a frequency of 0.8 Hz, is largely overestimated (the experimental to numerical power ratio is approximately equal to 0.6). The tests have been performed near the resonance frequency of the system (about 0.8 Hz). Probably, in such conditions, with relatively larger response amplitude, problems may be observed in the analysis, particularly using potential flow methods and larger discrepancy between simulated and observed data may be detected. An overestimation of power output has been nonetheless observed on the whole set of tested frequencies.

Anyway, the results of the potential flow simulations represent qualitatively well the response of the system, but they aren't in a good agreement with respect to predicted power output. Even if the absolute value of the predicted power is overestimated, it seems acceptable to use potential flow simulations in order to compare different configurations, considering the results only in a relative sense.

4 OPTIMIZATION BASED ON POTENTIAL FLOW SIMULATION

A numerical optimization procedure has been implemented in order to search a suitable system configuration for a given sea condition. To perform the optimization, the commercial code ModeFrontier, by ESTECO SpA, has been used in cooperation with Umbra Cuscinetti SpA.

The assumed sea state is extremely simplified and is assumed to be representable by a monochromatic wave of given frequency and amplitude. This approach has been chosen for design purposes in order to reduce the amount of simulation time, during multiple simulation runs, and the complexity of an irregular sea state. It has to be noted, however, that this is a

strong approximation and that the effect of irregular waves may have a significant impact on the final effective power output.

The optimization process has been applied to a system with the dimension of a possible real scale prototype, with a width fixed to 5 m, a length of about 3 m and a submerged volume of about 4 m^3. The width of the buoy was fixed to account for possible limitation on the available installation site and/or on the number of installable systems.

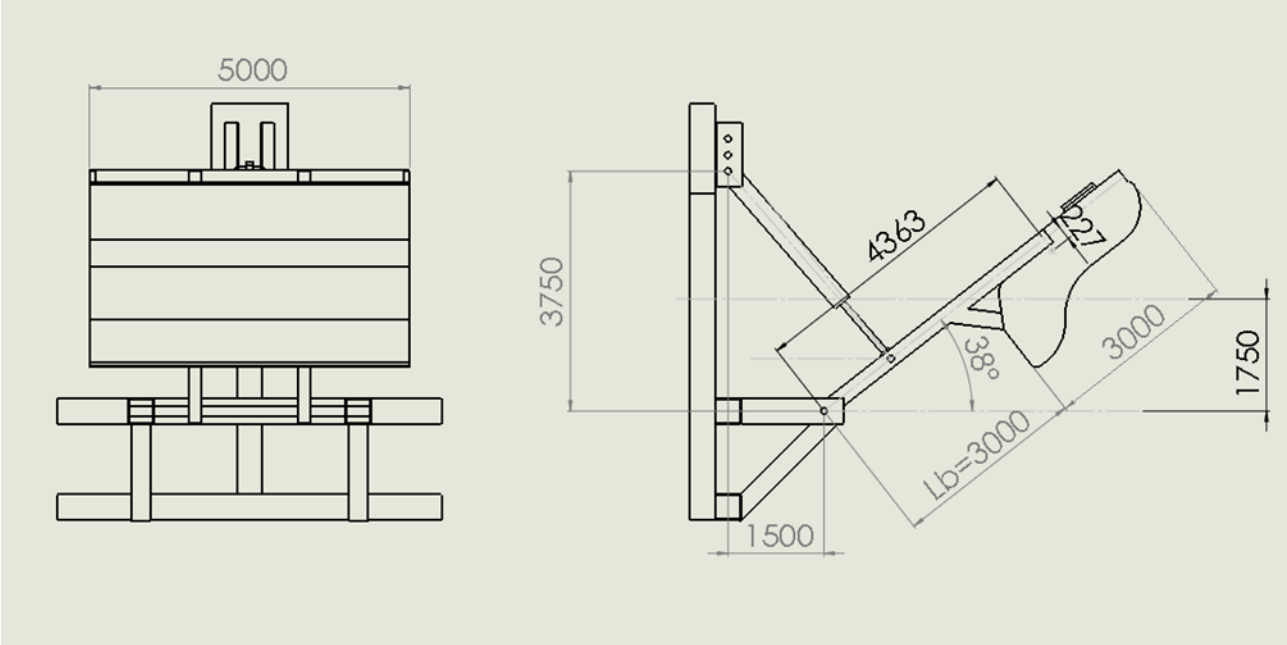

Figure 8: Dimensions of a possible real scale prototype. (Schematic only, the effectively model representation implemented in the code is simplified).

In the search process, for every examined configuration, a shape is generated and an initial equilibrium condition is found. With respect to this equilibrium condition a linearized hydrodynamic analysis is performed. A surface mesh is generated for the geometry, that is split into two parts distinguishing between diffractive (underwater) and non-diffractive elements. The radiation and diffraction problems are solved to obtain the related hydrodynamic coefficients (added mass and radiation damping, for radiation problem, and diffractive forces coefficients) for just the frequency of interest. Assuming a regular monochromatic wave, in the analysis of the radiation forces the convolution method, more proper for irregular seas, has not been used and the radiation forces have been estimated using the response amplitude operators and the hydrodynamic coefficients related to the prescribed incoming wave frequency.

A time domain simulation is then performed using the linearized coefficients previously estimated for the frequency of the incoming wave, together with a non-linear estimation of the hydrostatic and Froude-Krylov forces, which are calculated at each integration time-step considering the actual wetted surface. During time simulation the mechanical non-linearity due to the effect of the hinge and of the pivoting generator piston are taken into account. Power output is estimated by post-processing time simulation results. A schematic

representation of the process is reported. The algorithm will stop when it cannot find solution with better improvements than an assigned convergence value.

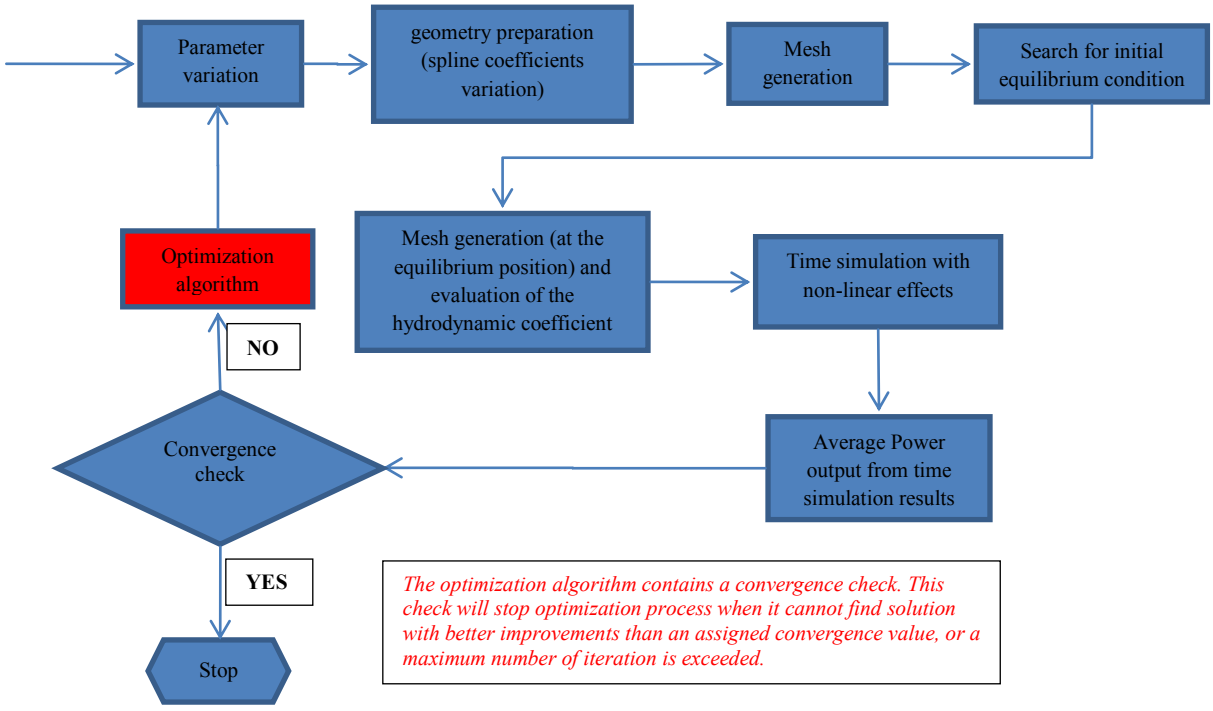

Figure 9: Optimization scheme

The following parameters have been accounted for in the optimization process:

- body mass (related to submerged volume at initial equilibrium condition)
- PTO force-speed gain
- body shape

The position of the center of gravity is assumed to be constant together with the assumed principal moment of inertia. Only the overall mass of the body is changed through the optimization process.

The geometry of the PTO connection, involving the length of the support arms and the position of the piston attachment points, is leaved unchanged. A linear PTO control law is chosen, defined by the value of the gain relating speed and generator required force (see Eq. (2)). The value of such gain is varied throughout the optimization process.

With respect to the shape of the body, only the cross-section shape is varied, leaving unchanged the transversal length in order to fulfill possible size constraints (for example, due to the available site extension). In a preliminary set of analyses the shape of the body was varied starting from an original shape constructed by means of circular arcs and straight lines. Only the forward part of the body facing the incoming wave is varied. In a second phase a B-spline curve, defined by 15 coefficients, is used to parameterize the cross-section shape of the body. In order to reduce the number of optimization parameter, only 3 coefficients are varied,

changing only the forward part of the body, which is supposed to be more influent in determining the interaction with the incoming wave. An initial shape has been chosen and a spline is approximated to such starting guess. The final result, found by the optimization algorithm, has shown a dependency on the choice of the initial shape. In general it is hard to state if there should be a single absolute optimal configuration for given conditions.

Some problems may arise using such approach to geometry representation: the parameters are not directly related to some geometric easily controllable parameter (such as a radius of a fillet) and some uncontrolled unsuitable shape may be reached during the process. This issue may be limited, but not completely solved, by choosing an initial shape (in this case the starting point was the shape of a buoy of a previous project) and the shape optimization parameters are given as limited increments to the starting configuration.

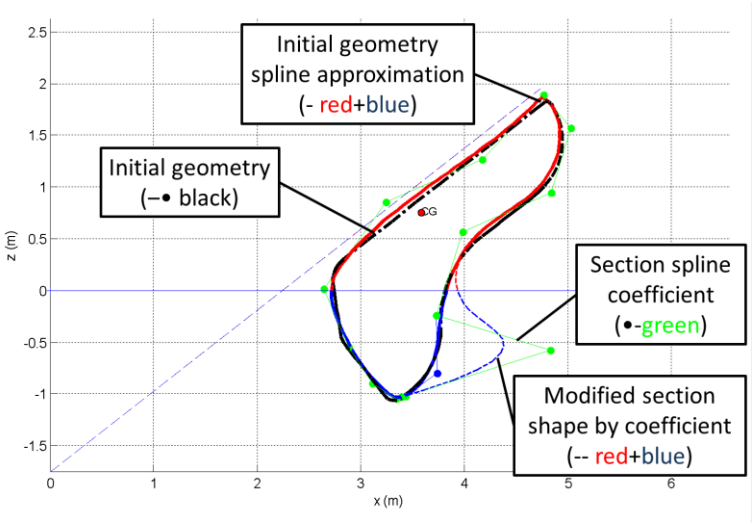

Figure 10: Section shape spline representation and modification

During some preliminary runs the body was also scaled in overall size, significantly changing the total mass and submerged volume. Volume change has shown a significant effect on power output. In order to observe the effect of the shape with limited size variation, the last optimization runs have been performed imposing a constraint on the maximum submerged volume.

For the particular case study under examination the width, in sense orthogonal to wave direction, is equal to W=5 m and the initial submerged volume is approximately equal to 4 m^3 and with an estimated weight of about 3780 kg. The optimization is performed for a wave with amplitude A_w=0.85 m and a period T_w=10 s. The wave model adopted is the Airy linear wave model.

The optimization algorithm used is the Nelder & Mead Simplex algorithm, which operates an exploration of the parameter space by modifying the vertex of a simplex (a set of n+1 points in the parameter space, where n is the number of parameters) through repeated basic operation (scaling, contraction, reflection) until convergence or for a limited number of runs. The target objective function is defined by the calculated average output power, which is estimated considering the mean of the instantaneous output power on the last 5 cycles, in

order to remove the possible effects of initial transients.

The final shape obtained by the optimization process show an effective increase in power output of about 29%. The final shape has a volume similar to that of the initial configuration, but with an increased cut water area. The initial starting equilibrium angle is also changed in the final configuration. Such trend in the geometry variation may be interpreted considering that, probably, the hydrostatic and Froude-Kryklov forces, which are related to the immersed volume and to the cut water area, seem to have a major effect on power output at least in the operating condition under exam.

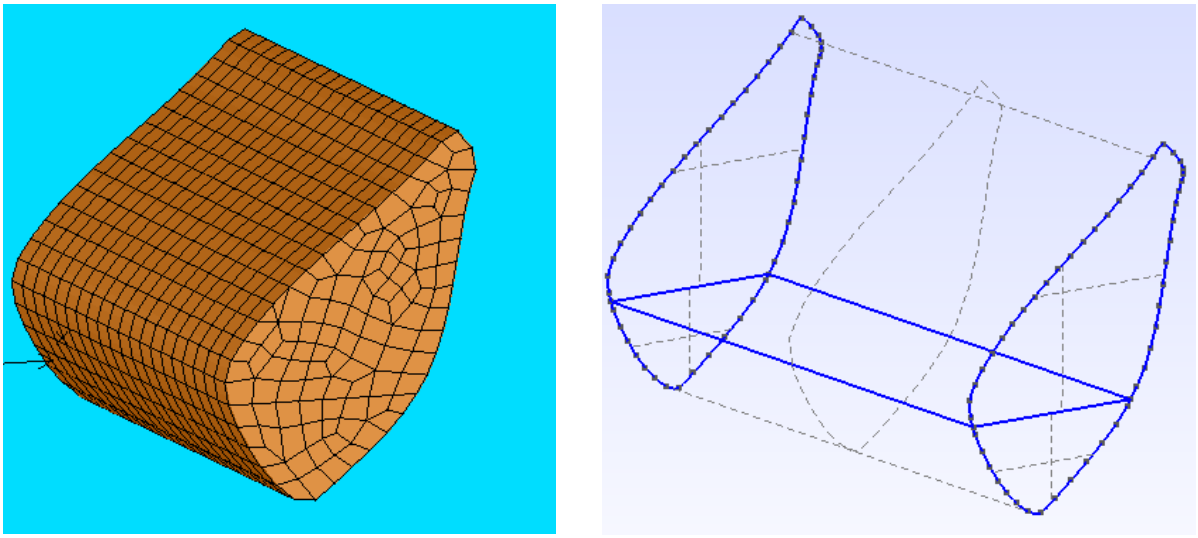

Figure 11: Mesh and geometry of the optimized shape. The mesh has 1014 elements

Table 3: Case study optimization results

	Search Method	K_{pist} (N/m/s)	Mass (kg)	P avg (kW)	Submerged Volume (m^3) (based on mesh)	Equilibrium angle (deg)
Modified configuration	Simplex method – 3 shape control variable	$5.25x10^5$	4040	8.0	~4.0	41.7
Initial configuration	Simplex method – 3 shape control variable	5.0x105	3780	6.2	~4.0	38
				Increment 29 %		

A different geometry, obtained in this particular case with a slight variation of the initial shape, seems to yield the same average power output increment with a different shape. The submerged part of the body is similar in both the solution, and the difference is limited to the above water portion of the body, which seems to have a minor effect on power output.

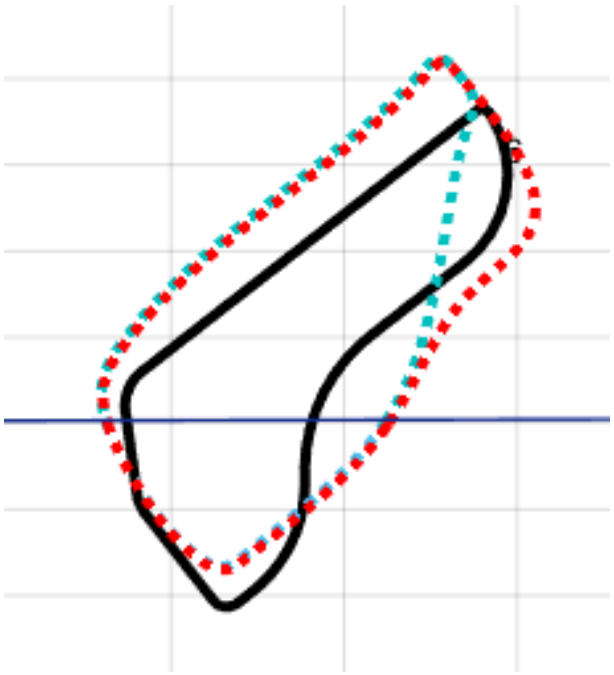

Figure 12: Comparison of two shapes (green and blue) with approximately the same power output increase. For reference the initial shape is reported (black).

6 RANS SIMULATIONS

Several Unsteady Reynolds Averaged Navier-Stokes (URANS) simulations were performed on the buoy only configuration, that is without connecting arms. These simulations were made to try to take in account viscous effects due to buoy movements into water. Due to symmetrical properties of the problem, only one half of the real physical water tank was reproduced. In the simulated wave/towing tank, the buoy can rotate around a non-physical hinge due to wave's actions. Different computational grids were tested and one was chosen which assure the better combination of accuracy and CPU time. In general, grids have a background and a superimposed grid, overset or chimera grid, which allows the buoy floating movements: the buoy is completely contained on the overset grid. Probably, the chosen mesh not ensures the best results in terms of absolute values, but it can be useful for trend analysis purposes. Each URANS simulation runs for about 30 s of simulation time, requiring about two days on a 64 CPUs device. Different turbulence models were also tested and k- ω model was chosen.

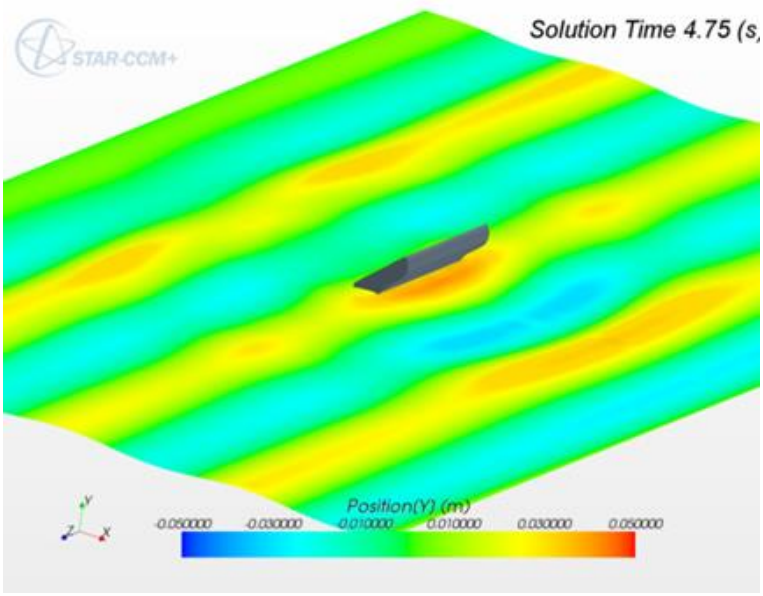

Figure 13: Typical RANS simulation screenshot

During simulations, data about hinge rotational angle and center of gravity (CG) position were recorded and used to evaluate mean and max available power. In the URANS simulations, effects of PTO device were also accounted for, in a way similar to that used in the potential flow simulations: the software used allow defining reference frames in which the user can evaluate some field functions, such as position, pressure, velocity, etc. In this way, defining a reference frame in the PTO anchor point, it is possible to measure velocity of the PTO anchor point due to buoy motion, along a prescribed direction. The velocity, normal to the supporting arms, was continuously evaluated during the simulation. Then, assuming a linear control law for the PTO (see Eq. (2)), the squared velocity was multiplied with the PTO control gain (k_v) in order to measure all the available power to the PTO. So, this available power was used as a reference for evaluating PTO control performance with respect to variations of its control gain. Several simulations were performed changing the k_v values in order to determine the best one for higher power extraction.

In Figure 13 is shown a single screenshot of the time evolution of the simulation. Observing time evolution it was observed that overall system dynamics is well reproduced, accordingly with that observed during test experiments. However, data about available max and mean power don't match sufficiently well the values measured during tests. The reasons of these are still unknown, but probably these have to be recognized to some mesh issues: indeed, it is known that mesh variations, due to refinements, has to be smooth and, if it is not, they can produce spurious and unphysical waves, which influence numerical solution.

In light of this, free-response simulations were performed and results had shown an underestimation of the natural frequency: natural frequency from URANS is about at 0.6 Hz, a bit lower with respect to both tests and potential flow simulations. Frequency response of the system was evaluated running simulations with monochromatic waves (single simulation for each frequency of the wave, while the wave amplitude was kept fixed) and evaluating power for each of them. The simulated frequency response had revealed that maximum

instantaneous and average power will occur at the same frequency as before. Sensitivity of the model about inertia and boundary condition variations was also analyzed without significant effects.

Other simulations were performed introducing the other frame structural elements around the buoy (supporting arms): these simulations highlighted that these elements seemed to produce no relevant changes of the system behavior with respect to its critical parameters.

7 CONCLUSIONS

- In this paper, it is presented a numerical analysis of a pivoted floating buoy for wave energy conversion. Numerical analysis have been performed with the aim of defining a suitable simulated wave/towing tank in order to investigate the shape and mass modification effects to optimize the system performances. As a reference, data from experimental tests have been used. The experimental tests have performed in the wave/towing tank facility of Department of industrial Engineering of University of Naples "Federico II".
- Numerical analyses have included potential flow simulations as well as URANS based calculations. Free response and frequency response to waves have been evaluated, showing a qualitatively acceptable agreement between potential flow simulations and available experimental data, although significant quantitative differences have been found in terms of power output.
- Due to its lower computational cost, the potential flow model has been chosen for optimization purposes: a shape optimization procedure has been set up and carried out, in order to maximize power production complying with assigned constraints. The optimization process was able to find a final shape with enhanced power output. Some dependence on initial guess shape has been observed. During the optimization process the shape of the section was varied together with buoy mass and force speed gain for fixed wave conditions. With the optimization procedure, a modified configuration has been identified that allows an average power improvement of about 29%, with almost the same submerged volume.
- Also URANS simulations have not shown a good quantitative agreement with test data. Probably, this is due to mesh issues, so further investigations are needed. Despite this, the simulated behavior of the system under wave action seems to reproduce very qualitatively what has been observed during tests. Nevertheless, the real impediment to use URANS as an optimization tools is the huge computational duty, with respect to potential flow simulations.

REFERENCES

[1] D. P. Coiro, G. Troise, U. Maisto and G. Calise, "Numerical And Experimental Tests On A Scaled Model Of A Point Pivoted Absorber For Wave Energy Conversion", 2nd Asian Wave and Tidal Energy Conference (AWTEC), Tokyo, 2014.
[2] M. McCormick, "Ocean Engineering Wave Mechanics", Wiley-Interscience, (1973).
[3] M. McCormick, "Ocean Wave Energy Conversion", Dover, (2007).
[4] G. De Backer, "Hydrodynamic Design Optimization of Wave Energy Converters Consisting of Heaving Point Absorbers", Ghent University, (2009).

[5] H. O. Berteaux, “Buoy Engineering”, Wiley-Interscience, (1976).
[6] Matsuoka et alii, "A Study of Wave Energy Conversion Systems Using Ball Screws - Comparison of Output Characteristics of the Fixed Type and the Floating Type", Proceedings of The Twelfth International Offshore and Polar Engineering Conference, (2002).
[7] O.M. Faltinsen, “Sea loads on ships and offshore structures”, Cambridge University Press, (1990).
[8] G. Payne, “Guidance for the experimental tank testing of wave energy converters”, SuperGen Marine, (2008).
[9] CD-adapco, “User Guide STAR-CCM+ version 7.06”, (2012)